The role of Cav3.2 channels in noise-induced hearing loss

Kriti Rajda[1]

Supervisors: Dora Persic[2], Sonja Pyott[2]

[1]N-Track, Research School of Behavioural and Cognitive Neurosciences, Faculty of Science and Engineering, University of Groningen.

[2] Department of Otorhinolaryngology, Universitair Medisch Centrum Groningen.

Abstract

The prevalence of noise-induced hearing loss (NIHL) has been growing since the onset of the 21st century. The molecular pathology of NIHL is not yet well-known; previous research points to dysregulation of calcium homeostasis in the inner ear being an important cause. In this study, we focus on the role of calcium and its influx via the Cav3.2 ion channel in cochlear function and response to noise exposure.

Voltage-gated calcium channels (VGCCs) have an α-subunit with ten possible isoforms. In this study, we focus on the Cav3.2 isoform, encoded by the CACNA1H gene, prominently expressed in the cochlea and auditory brainstem. Earlier studies show that Cav3.2 knockout (KO) mice at five months show elevated auditory thresholds compared to wild type (WT) mice; therefore, this gene may also be essential for the normal hearing process. However, considering the advanced age of the mice in those studies, absence of this channel may merely accelerate age-related hearing loss; therefore, younger knockouts must be tested.

The current study examines effects of noise exposure on CACNA1H KO and heterozygous (HET) mice at six weeks of age. This was done through a combination of auditory brainstem response (ABR) studies on WT, KO and HET mice, in baseline conditions, 24 hours after noise exposure, and at 7-day and 14-day intervals after noise exposure. At baseline, KO mice had elevated auditory thresholds, lower wave I amplitudes and higher wave I latencies, meaning their hearing is impaired by loss of Cav3.2. Meanwhile, after noise exposure, the differences were not as pronounced, but hearing was significantly worsened from the baseline in both WT and KO mice. The cochleae were dissected and immunostained before imaging with confocal microscopy and counting inner hair cells and associated synapses. No significant differences were seen between the synapse or cell densities of WT and KO mice (HET mice were not morphologically examined).

The current conclusions of the study are that absence of both copies of the CACNA1H gene impairs hearing and affects the extent to which noise exposure damages it, making KO mice more susceptible to hearing impairment. However, the damage is usually lessened in heterozygous mice.

Introduction

Prevalence and pathologies of excessive noise exposure

In recent years, the levels of ambient noise in the world have been increasing. The average level of noise a person is exposed to on a daily basis in the modern day is also far higher than in previous centuries[1]. A survey conducted across the years 2003-04 estimated the prevalence of speech-frequency hearing loss in adults aged 20-69 as approximately 16.1%, and in age groups 20-29 as 8.5% and steadily growing[2]. Various factors may increase the risk of developing hearing loss. For example, men are 5.5-fold more likely to experience hearing impairment than women. Additionally, smoking, cardiovascular risks and noise exposure also increase the likelihood of hearing loss[2].

Many studies since Kryter et al (1966)[3] have proven that prolonged exposure to noise results in temporary as well as permanent damage to hearing. The most obvious indicator of this is a shift in auditory threshold, i.e., the minimum sound level of a pure tone that an average human is able to hear when no other sound is present. Prolonged noise exposure leads to first a temporary and then a permanent shift in the auditory threshold of the exposed individual[4].

Apart from permanent auditory threshold shifts, another pathology of noise exposure visible in post-mortem tissue is synaptopathy, or the loss of synapses between inner hair cells (IHCs) and auditory nerve fibres. Synaptopathy disrupts connections between the cochlea and the central auditory system, and it is known to impair speech perception in environments with high levels of background noise, as well as increase the likelihood of tinnitus and hyperacusis[5]. It is also known that excessive noise exposure can lead to the death of outer hair cells (OHCs)[6], most severe in the 9 mm to 13 mm region of the cochlear duct[7].

Noise exposure is also associated with various pathologies of OHCs, IHCs and spiral ganglion neurons (SGNs). One of these pathologies is cochlear inflammation. Damage to OHCs due to noise exposure leads to activation of damage-induced molecular patterns (DAMPs), whose receptors are present on cochlear cells; binding of DAMPs to their receptors leads to the release of pro-inflammatory cytokines and chemokines[8]. However, the molecular mechanisms of noise-induced hearing loss have not yet been fully resolved.

Role of calcium in noise-induced hearing loss

Noise exposure-induced cell death also leads to the generation of free radicals or reactive oxygen species (ROS) in the cochlea[9] and increased calcium levels in the endolymph and hair cells[10]. Several routes for Ca^{2+} influx into the cytoplasm have been documented (Fig. 1). Suggested causes for the increase in calcium concentration in OHCs include an entry from extracellular compartments through L-type Ca^{2+} and P2X2 ATP-gated channels. Further, a positive feedback loop appears to be created with the entry of calcium from extracellular compartments, enhancing the release of Ca^{2+} from intracellular compartments further. This influx of calcium leads to an overload of calcium ions and toxicity inside OHCs[11].

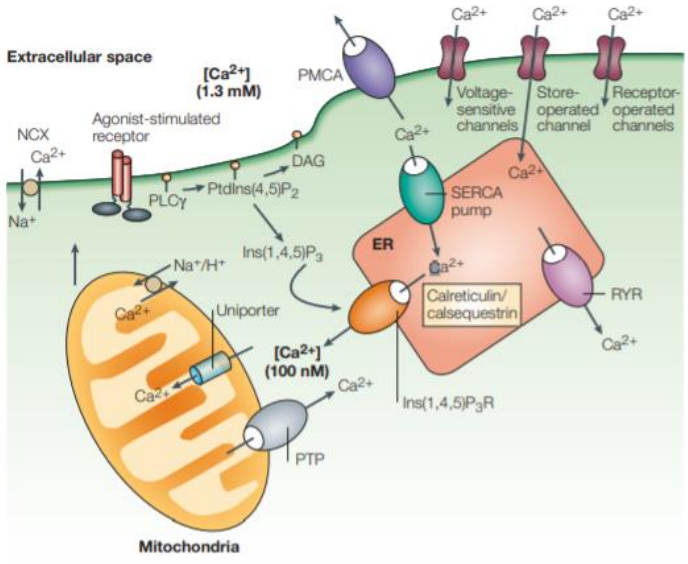

Fig. 1: Regulation of intracellular calcium compartmentalization[10]

While calcium appears to play a role in noise-induced hearing loss, it is not yet well-defined. It is known that exposure to loud sound leads to excitotoxicity in SGNs, with the noise triggering excessive release of glutamate from IHCs[12]. A specific class of glutamate receptors, i.e., Ca^{2+}-permeable α-amino-3-hydroxy-5-methylisoxazole-4-propionic acid receptors (CP-AMPARs) appears to be majorly responsible for this excitotoxic trauma; thus, activation of CP-AMPARs through calcium influx is one of the mechanisms responsible for noise-induced

synaptopathy[13]. It was previously shown that overstimulation through sound could lead to both an excessive influx of calcium[10] and activation of certain mitochondria-mediated cell death pathways in OHCs[14]. It was also known that the release of glutamate further leads to an entry of calcium from extracellular compartments into outer hair cells[15]. Thus, the role of calcium in triggering mitochondria-mediated death pathways was studied, and it was found that calcineurin activates Bcl-2-associated death promoter (BAD), which translocates to the mitochondria in degenerating cells[14].

Voltage-gated calcium channels in the inner ear

It thus follows that controlling the release of calcium upon noise exposure might aid in resisting or mitigating its effects on hearing loss. Therefore, research attention becomes focused on voltage-gated calcium channels (VGCCs) in the inner ear, their localization and function. VGCCs or Cav channels are macromolecular complexes comprising several subunit proteins. The central and pore-forming subunit is known as the α-subunit and may have one of ten different isoforms. Other structures that contribute to this complex include β-subunits (with one of four possible isoforms) and one of four possible $\alpha_2\delta$ subunits[16]. Eight of the known α-subunits of these channels have been found to be expressed in the inner ear. Some α-subunits (Cav1.2, Cav2.3, Cav3.1) were also immunolocalised to Schwann cells[17].

The Cav1.3 isoform of the α-subunit is the most abundantly expressed in the inner ear, especially by inner hair cells. This subunit is encoded by the CACNA1D gene. Expression of this gene is observed to be about three-fold greater at the RNA level and two-fold greater at the protein level in OHCs as compared to IHCs[18]. Knockout mice for this gene show almost complete deafness while heterozygous mice show significantly elevated auditory thresholds; thus, it can be concluded that this VGCC is essential for functional hearing[19]. Additionally, histopathological studies of knockout mice showed that inner and outer hair cells underwent degeneration and there was a complete absence of L-type currents evoked in the inner ear, leading to congenital deafness[20]. A functional Cav1.3 channel subunit in the inner ear is required for both the growth and development of hair cells, efficient glutamate release during synaptic transmission, and generation of Ca^{2+}-evoked action potential[21]. The Cav2.3 channel has also been known to be expressed in the developing and adult mouse organ of Corti, specifically in the basal poles of the outer hair cell membranes in adult mice[22].

The Cav3 family of calcium channels (encoded by the CACNA1G, CACNA1H and CACNA1I genes), also known as the T-type calcium channels, are normally responsible for the regulation of neuronal excitability[23]. Genetic tracing has found that Cav3.2 is predominantly expressed in the dentate gyrus of the hippocampus, as well as in many mechanoreceptor and nociceptor endings[24]. Due to their highly conserved amino acid sequences, as well as a lack of availability of channel blockers specific to each subunit, it has been difficult to resolve specific roles of each of the individual channel family members.

There is evidence for the presence of these channels in the outer hair cells of rats. PCR experiments established the expression of Cav3.1 channels, but not Cav3.2 or 3.3, in the mature rat cochlea. Through immunohistochemistry and hybridisation experiments, it was found that Cav3.1 is expressed in both the inner and outer hair cells at the mRNA level, but only in outer hair cells at the protein level[24]. Cav3.2 is known to be the most prominently expressed subgroup of auditory calcium channels in the cochlea and auditory brainstem[25]. Little is known about expression of the Cav3.3 channels in the sensorineural structures of the inner ear.

As the Cav1.3 channel has been established to be the indispensable VGCC for functional hearing, it may not be useful to conduct further studies on these knockout mice. Instead, it may

be beneficial to study the role of the other Cav channels in hearing further, and in this particular study we focus on Cav3 channels specifically.

Role of Cav3 channels in hearing

Auditory brainstem response tests (ABRs) performed on five-month-old Cav3.2 wildtype (WT), knockout (KO) and heterozygous (HET) mice showed that KO mice exhibited elevated auditory thresholds at five months of age. In addition, there were significant variances in amplitudes and latencies of the first wave in the ABR response, indicating that the Cav3.2 channel may play a more important role in hearing than was earlier thought. In WT and HET mice, the auditory threshold for click-based audio responses was closer to 40 dB, while in knockout mice it was around 65 dB. Amplitudes of wave I in the knockout mice was lower, while the latency was higher[26]. However, it is important to note that these mice are slightly older and the lack of the CACNA1H gene may also have accelerated age-related hearing loss. Hence, it is not yet clear whether expression of this gene is essential to hearing at a younger age, or how it alters susceptibility to noise-induced hearing loss.

Current hypothesis and proposed experiment

In this work, we hypothesized that Cav3.2 KO mice would show protection from noise-induced hearing loss because they lack a route of Ca^{2+} influx to trigger excitotoxic damage. In the current study, the effects of noise exposure on hearing in Cav3.2 KO mice have been studied, as well as the auditory phenotype of KO and HET mice at younger ages (approx. 6-8 weeks) pre- and post-noise exposure. The aim of this study is to assess whether the lack of Cav3.2 channel, whether total (as in KO mice) or partial (as in HET mice), provides protection against noise-induced hearing loss. Therefore, the hearing of WT, KO and HET mice is expected to be very similar prior to noise exposure, and after, KO and HET mice are expected to have better hearing than WT mice.

Materials and Methods

Animals: CaV3.2 heterozygous (HET) mice were obtained from Prof. Dr. Pernille B. L. Hansen (University of Southern Denmark) and were bred on a C57BL/6 background. Upon crossing CaV3.2 HET mice with each other, CaV3.2 knockout (KO) mice (n=11) were obtained and crossed to maintain KO breeding lines. CaV3.2 KO mice were compared to wild-type (WT) mice (n=6) of the same strain obtained from the UMCG CDP. HET mice (n=6) were also later bred from KO and WT mice.

Assessments of cochlear function: Auditory brainstem response (ABR) measurements were used to quantitatively assess cochlear function in response to both clicks and pure tones (8, 16, 24 and 32 kHz) using procedures described in more detail below (Fig. 2)[27]. ABR was first described by Jewett and Williston in 1971[28]. It measures the capacity of a test subject to generate an evoked auditory potential when either a ‘click’ sound or a tone pip is transmitted to their ears in open field conditions (i.e., the speaker that transmits the noise is placed 10cm from the ears of the test subject). The elicited waveform is measured through electrodes wired to the scalp. The auditory threshold is the lowest volume at which a waveform is detectable.

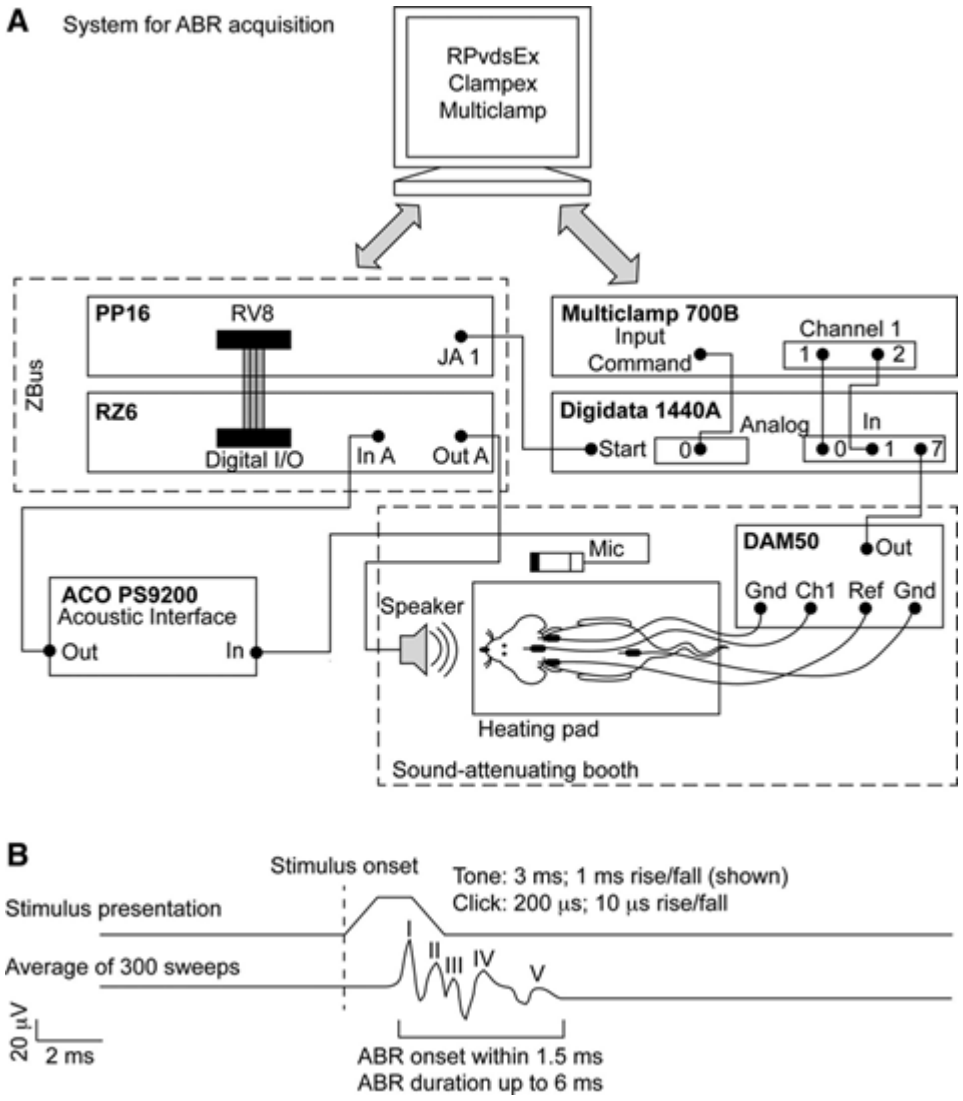

Fig. 2: A. A diagram of a typical setup for ABR measurements of mice in an open field setup[29], with electrodes attached to the mouse's earlobes and forehead. The mouse is sedated while placed in the soundproof chamber, and as it is unconscious, it is placed on a heating pad to retain body heat. Sounds are played through the speaker and the waveform generated by the auditory brainstem is visualized through a script run through SmartEP software. B. A typical waveform of an ABR, along with waves I-V of the auditory response.

ABR measurements were performed on WT, KO and HET mice at different time points beginning from the age of six weeks in baseline conditions. Mice were sedated using a mixture of ketamine (75 mg/kg) and xylazine (100 mg/kg). When they were fully unconscious, they were placed inside a soundproof chamber, electrodes were subdermally attached by the earlobes and at the back of the head, and they were exposed to pure tones (8, 16, 24 and 32 kHz) and clicks at increasing decibel levels (0 dB to 90 dB in 5-dB increments).

A baseline ABR reading was taken to determine their auditory thresholds, as well as amplitudes and latencies of wave I of the auditory response. One week after this measurement was taken, the mice were exposed to a consistent level of noise (70 dB) for two hours inside the soundproof chamber. After this, the mice were allowed to recover for a week, and then ABR was performed again to record the permanent threshold shift 7 days after noise exposure (PTS 7d). This process

was repeated again after a week to record the permanent threshold shift 14 days after noise exposure (PTS 14d).

The waveforms were visualized and observed by means of the SmartEP software, version 2.70, developed by Intelligent Hearing Systems (IHS). This software also allows for measurement of amplitudes and latencies of wave I of the waveform.

Immunofluorescence: Immunofluorescence was performed in the isolated sensory epithelium of the cochlea, the organ of Corti (i.e., the strip of epithelial hair cells in the inner ear that produces nerve impulses in response to sound vibrations) to quantify the IHC and OHC density and synaptic contacts between the IHCs and SGN. A description of these techniques can be found in more detail in other literature[30].

After the final ABR readings at the PTS 14d time point were taken, the mice were anaesthetized using isoflurane before being sacrificed by decapitation. Their cochleae were isolated from the temporal bones and immersed in phosphate buffer saline (PBS) solution. Following this, they were immersed in a fixate solution containing 4% paraformaldehyde (PFA) for 1 to 3 hours to fix the tissue. Complete organs of Corti were then isolated from the cochlea and treated with a blocking buffer (PBS with 5% normal goat or donkey serum and 0.2% Triton X-100) for 1 to 3 hours at room temperature. They were then incubated overnight in the primary antibody diluted with blocking buffer and rinsed three times in PBS with 0.2% Triton X-100 (PBT) for 20 minutes each time. After rinsing, the turns were incubated in the secondary antibody diluted in blocking buffer for 2 hours at room temperature before once again being rinsed three times in PBT and then once in PBS. They were then mounted on glass slides in Vectashield mounting medium (Vector Labs). All incubations and rinses were performed on a rocking table[31].

Various antibodies were used for immunofluorescent staining and to identify the sub-cellular localization of these channels. For immunofluorescent staining, the antibodies used included: mouse anti-CPBT2 (C-terminal binding protein 2), rabbit anti-prestin (a motor protein highly expressed in the OHCs), and mouse anti-GluA2 (a glutamate receptor subunit that regulates calcium permeability and trafficking of Ca^{2+}). The antibody used to identify localisation of Cav3.2 is the rabbit anti-CaV3.2 (CACNA1H; #ACC-025[32]. The secondary antibodies used for staining IHCs and presynaptic terminals were Alexa Fluor 488 (green fluorescence), while the OHCs are stained with Alexa Fluor 647 and appear red.

Low-magnification micrographs of the immunostained organs of Corti were taken using fluorescence microscopy. The Leica 4000b fluorescence microscope was used to take full images of each part of the cochlea that had been isolated. If full images of a particular section were not possible, partial images were stitched together using the Hugin software. Following this, Fiji Is Just ImageJ (FIJI) a modified version of the ImageJ-Win64 software (specifically the MosaicJ and Measure Line plugins, along with the previously determined frequency map of the mouse cochlea) was used to draw a tonotopic map of the frequency regions of the cochlea as an overlay to this image, which were then used when more detailed images were being captured.

After the maps were completed, the frequency regions of 8, 16, 24 and 32 kHz of each viable sample were imaged using the Leica sp8 confocal microscope. High magnification confocal micrographs were collected with a 63× oil immersion lens under the control of the LAS X

software. Z-stacks of the entire inner hair cell (IHC) synaptic pole from the 8, 16 and 32 kHz region were collected at a scan speed of 200 Hz and zoom of 1. The step size (optical section thickness) was determined by stepping at half the distance of the theoretical z-axis resolution (the Nyquist sampling frequency). Images were acquired in a 1024×1024 raster ($x = y = 184.52\ \mu m \times 184.52\ \mu m$) at sub-saturating laser intensities for each channel. Images are presented as z-projections through the collected optical stack. All quantitative image analysis were performed on the raw image stacks, without deconvolution, filtering, or gamma correction. If both organs of Corti of the mice were viable, images of both were taken. The sample that had as many frequency regions intact as possible was preferred in every case. Post-imaging, the number of inner hair cells and inner hair cell synapses at each frequency region were counted, and the numbers in wild type, knockout and heterozygous mice were compared.

Counting of inner hair cells and synapses was done on 3D reconstructions of the Z-stacks of the confocal image stacks using the Imaris 6.4 image analysis software. Here, the number of synapses per inner hair cell was calculated, as well as the density of synapses (i.e., the number of synapses per unit length – in this case, per micrometer).

Analysis: The absolute auditory threshold, the threshold shift that occurred between the baseline and each time point, the wave I amplitude at each volume increment and the wave I latency at each volume increment were analyzed and compared between KO, HET, and WT mice, using Microsoft Excel. Thresholds were determined using a custom-made R script.

Statistical analysis: comparisons between thresholds in WT, KO and HET mice done using Šidák's multiple comparison test on a mixed-effects model.

Results and Discussion

ABR data: auditory thresholds, amplitudes and latencies

The absolute auditory thresholds of WT, KO and HET mice showed some interesting variations from the predicted results. For instance, the baseline thresholds of all mice at the age of six weeks were expected to be fairly similar; as the lack of Cav3.2 channel was not expected to cause any defects in hearing at this age (Fig. 3A). However, in baseline conditions, the KO mice already had significantly higher auditory thresholds than either WT or HET mice in almost all conditions, excluding the 8 kHz condition where WT mice appear to have significantly lower thresholds than HET and KO mice.

After noise exposure, the hearing of KO mice continues to be majorly worse than WT or HET mice. In PTS 7d conditions (one week after noise exposure) KO auditory thresholds continue to be significantly higher in all conditions except 32 kHz tones, where there is no significant difference between KO, WT and HET thresholds (Fig. 3B). This worsening of hearing continues on into the PTS 14d conditions (two weeks after noise exposure), where there is no significant difference between thresholds of all three groups in any conditions (Fig. 3C).

The auditory thresholds of HET mice were measured in order to provide further clarity on this issue and to determine whether partial lack of the Cav3.2 channel provided protection against noise-induced hearing loss. The baseline thresholds for HET mice tended to be similar to WT mice, thus partial lack of the channel appears not to negatively affect hearing; however, post-noise exposure, thresholds of the two groups continue to be similar. This also suggests that partial lack of the Cav3.2 channel does not provide any significant protection against noise-induced hearing loss.

A

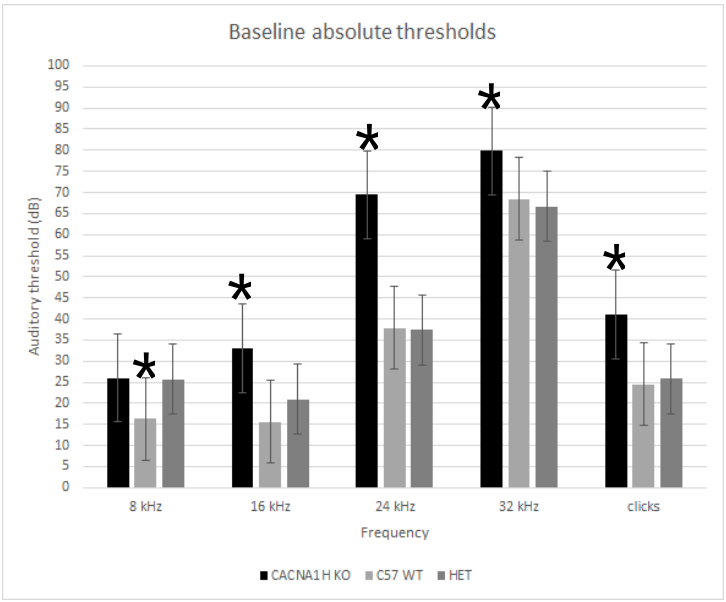
Baseline absolute thresholds
Auditory threshold (dB)
100
95
90
85
80
75
70
65
60
55
50
45
40
35
30
25
20
15
10
5
0
8 kHz
16 kHz
24 kHz
32 kHz
clicks
Frequency
CACNA1H KO
C57 WT
HET

B

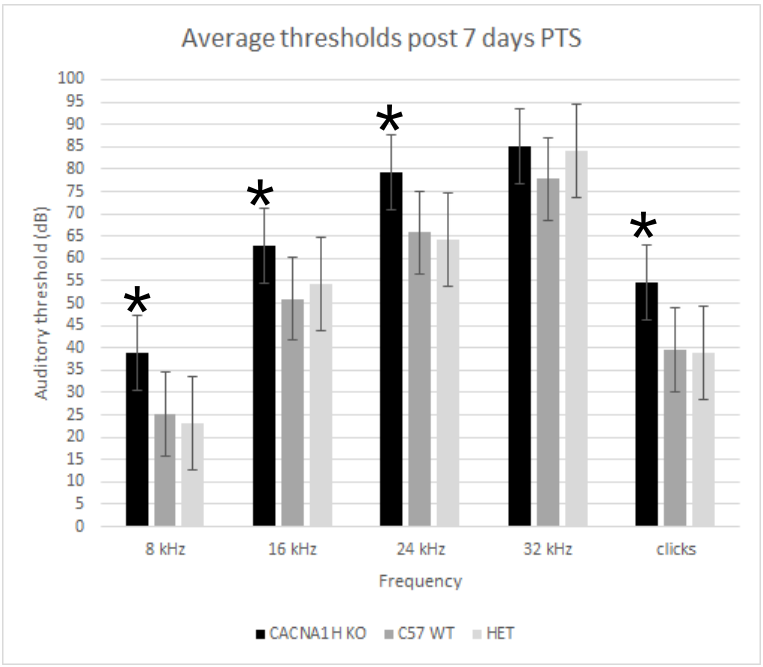
Average thresholds post 7 days PTS
Auditory threshold (dB)
100
95
90
85
80
75
70
65
60
55
50
45
40
35
30
25
20
15
10
5
0
8 kHz
16 kHz
24 kHz
32 kHz
clicks
Frequency
CACNA1H KO
C57 WT
HET

C

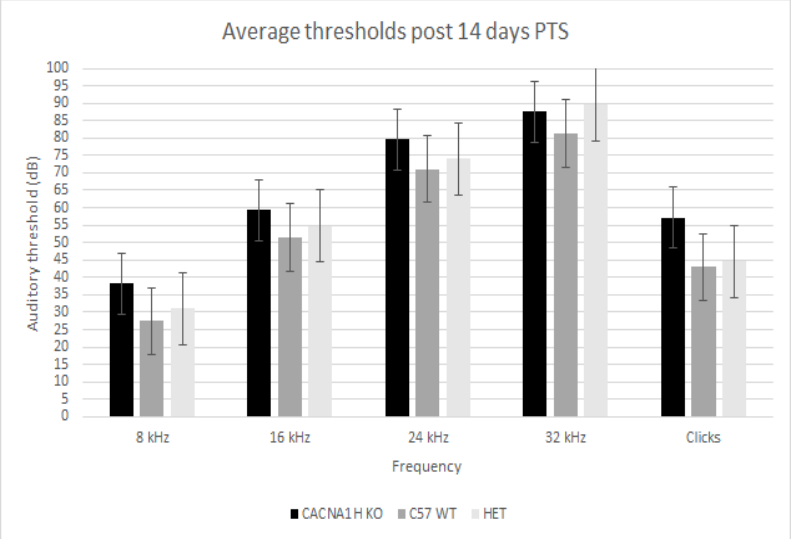

Fig. 3: Average auditory thresholds of Cav3.2 KO, HET, and WT mice taken at different time-points: A) baseline (before exposure to noise), B) 7 days post-threshold shift (PTS) (a week after exposure to noise) and C) 14 days PTS (two weeks after exposure to noise).

Amplitudes were examined in addition to absolute auditory thresholds in order to properly interpret the ABR data. The amplitude is directly correlated to the number of neurons firing in response to the sound stimulus. In baseline conditions, HET mice almost consistently have higher wave I amplitudes than either WT or KO mice, except in the case of 32 kHz, where WT mice have the highest amplitudes. However, KO mice consistently have the lowest amplitudes among the three groups of mice.

In one-week post-noising conditions, the KO amplitudes mostly continued to be lower than the WT or HET amplitudes. However, at lower sound intensities (up to about 40 kHz), amplitudes of all groups of mice were very close in value and any divergence in values occurred at higher sound intensities. Additionally, the WT and HET amplitudes show no noticeable trend of one being higher or lower than the other, and for click sounds (which register across frequency regions), these two average amplitudes are very close in value across all sound intensities.

In two-week post-noising conditions, the WT amplitudes appear to be higher than HET and KO amplitudes in almost all conditions, although the differences between the amplitudes of all three groups are much smaller in these conditions. However, KO amplitudes continue to be lower than those of WT and HET mice.

A

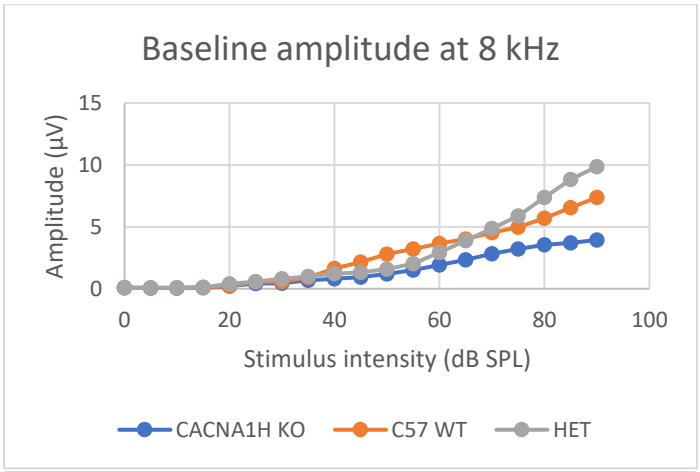
Baseline amplitude at 8 kHz
Amplitude (µV)
15
10
5
0
0
20
40
60
80
100
Stimulus intensity (dB SPL)
CACNA1H KO
C57 WT
HET

B

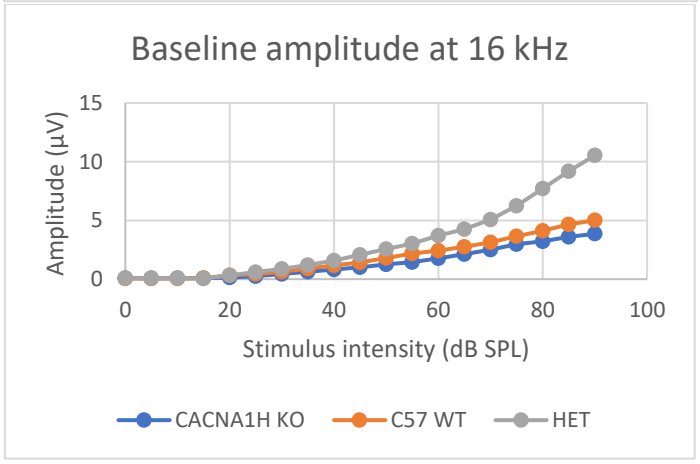
Baseline amplitude at 16 kHz
Amplitude (µV)
15
10
5
0
0
20
40
60
80
100
Stimulus intensity (dB SPL)
CACNA1H KO
C57 WT
HET

C

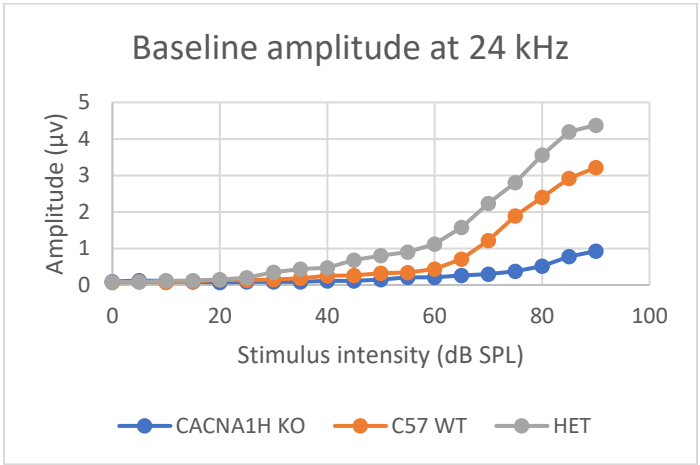
Baseline amplitude at 24 kHz
Amplitude (µv)
5
4
3
2
1
0
0
20
40
60
80
100
Stimulus intensity (dB SPL)
CACNA1H KO
C57 WT
HET

D

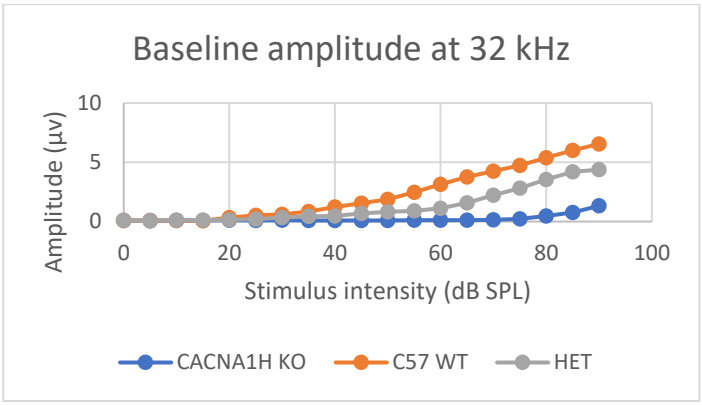

E

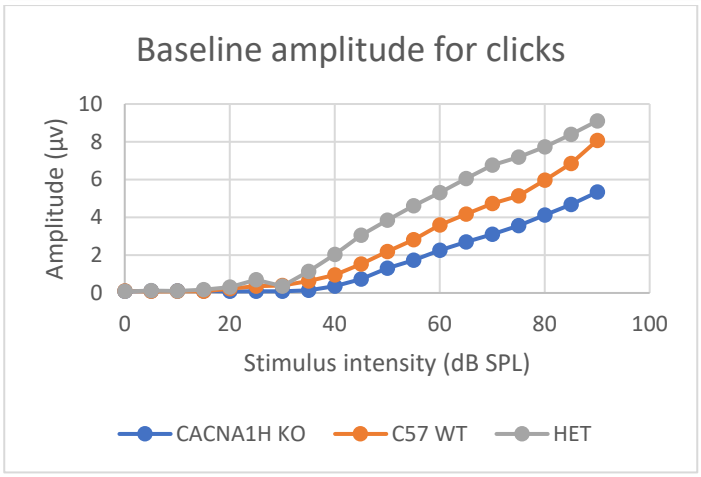

Fig. 4: Amplitudes of wave I of ABR responses of six-week-old mice in baseline conditions (prior to noise exposure) for various frequencies of pure tones. A: At 8 kHz, B: at 16 kHz, C: at 24 kHz, D: at 32 kHz, E: for click noises.

A

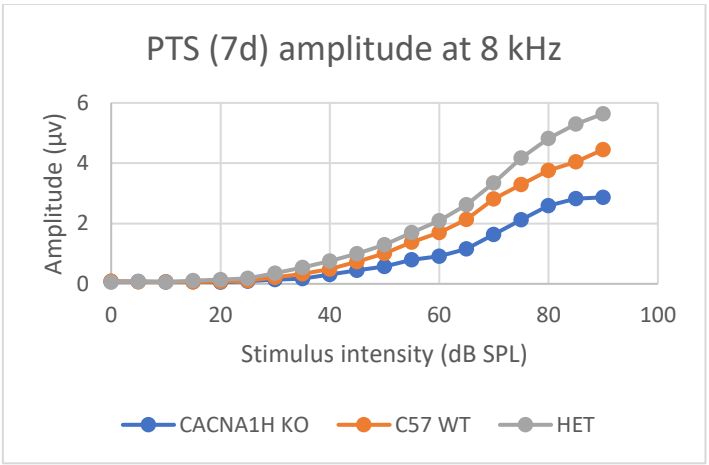

B

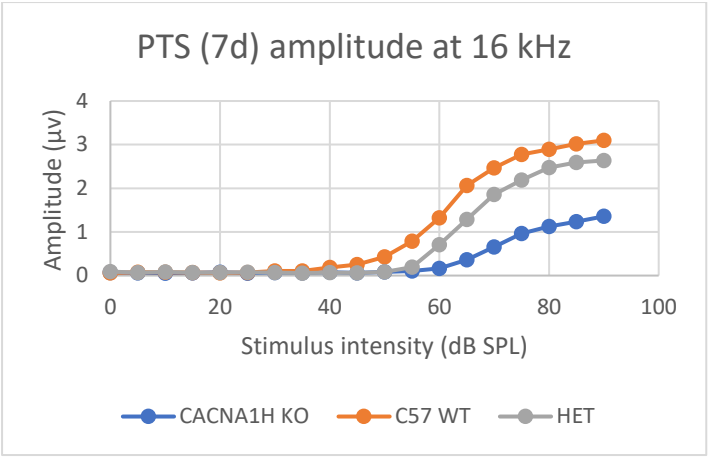
PTS (7d) amplitude at 16 kHz
Amplitude (µv)
0
1
2
3
4
0
20
40
60
80
100
Stimulus intensity (dB SPL)
CACNA1H KO
C57 WT
HET

C

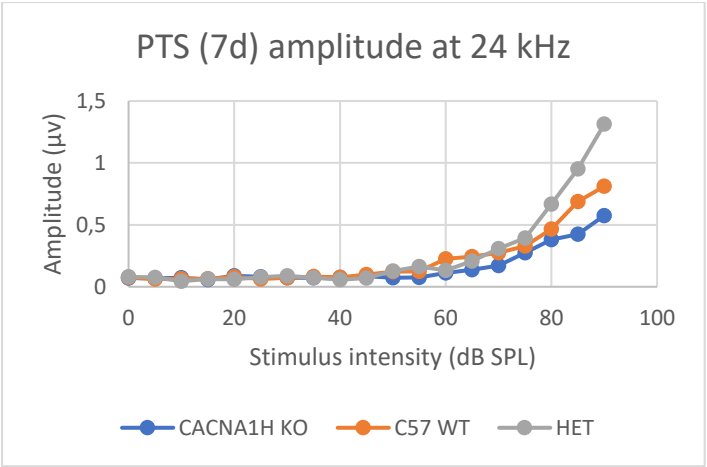
PTS (7d) amplitude at 24 kHz
Amplitude (µv)
0
0,5
1
1,5
0
20
40
60
80
100
Stimulus intensity (dB SPL)
CACNA1H KO
C57 WT
HET

D

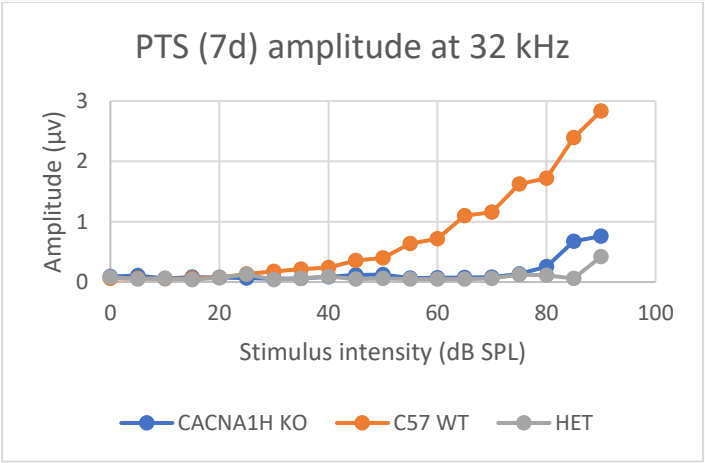
PTS (7d) amplitude at 32 kHz
Amplitude (µv)
0
1
2
3
0
20
40
60
80
100
Stimulus intensity (dB SPL)
CACNA1H KO
C57 WT
HET

E

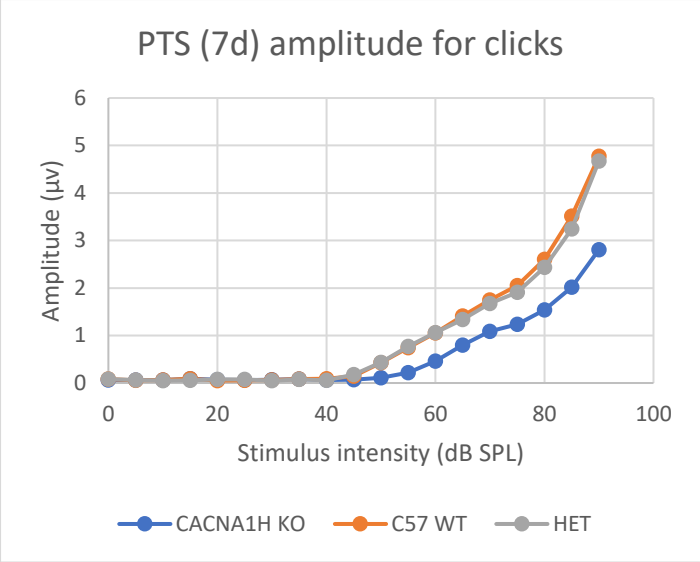

Fig. 4: Amplitudes of wave I of ABR responses of six-week-old mice in PTS 7d conditions (one week post noise exposure) for various frequencies of pure tones. A: At 8 kHz, B: at 16 kHz, C: at 24 kHz, D: at 32 kHz, E: for click noises.

A

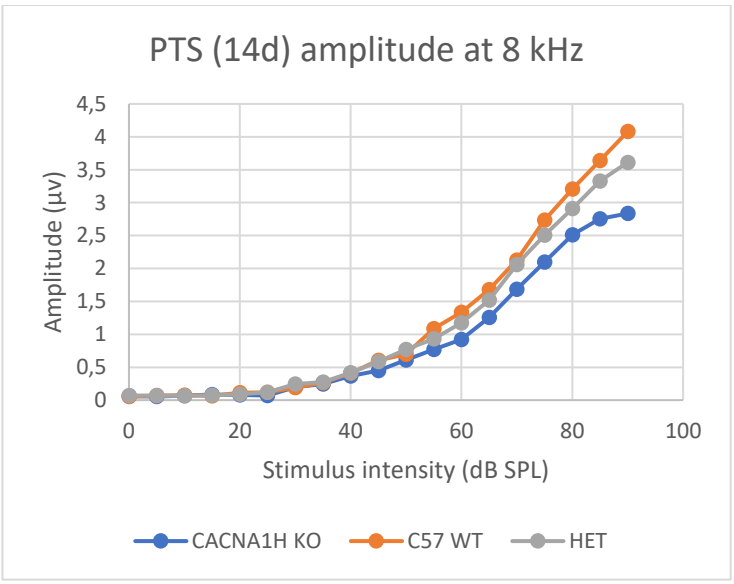

B

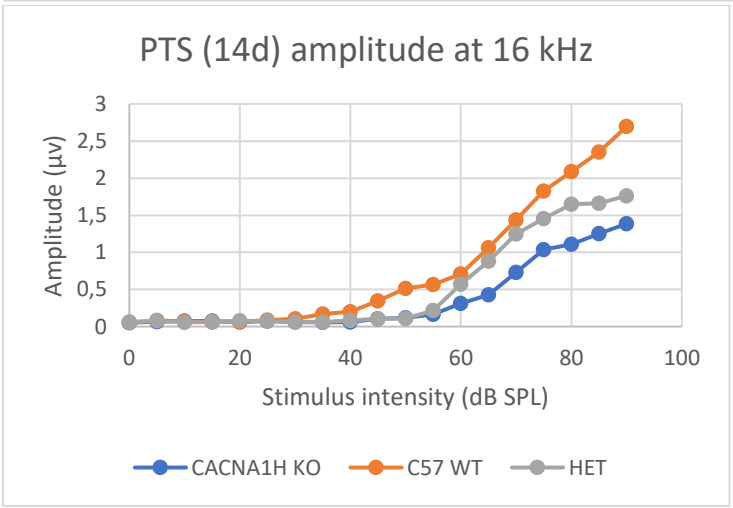

C

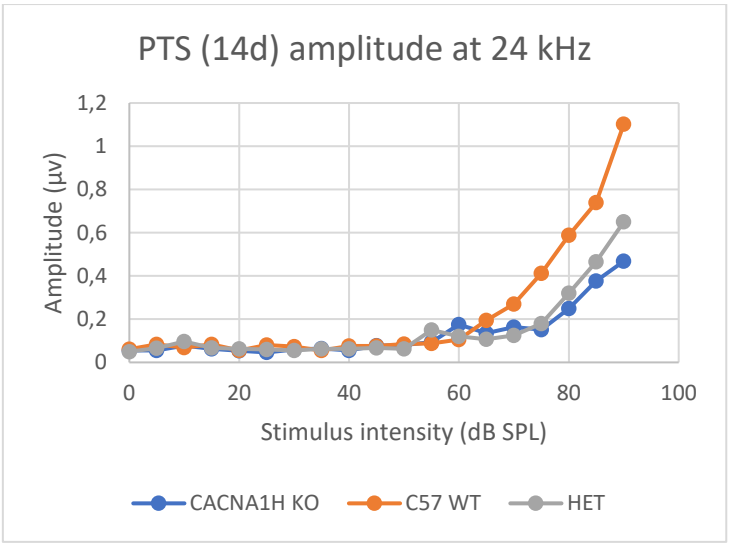

D

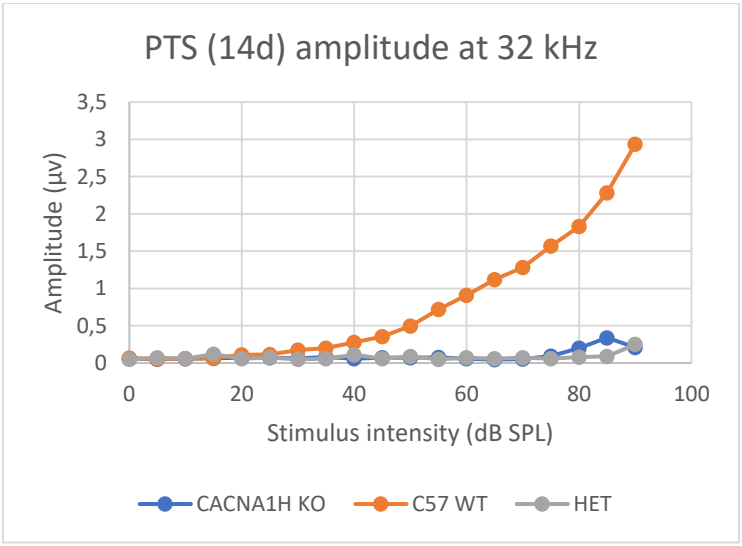

E

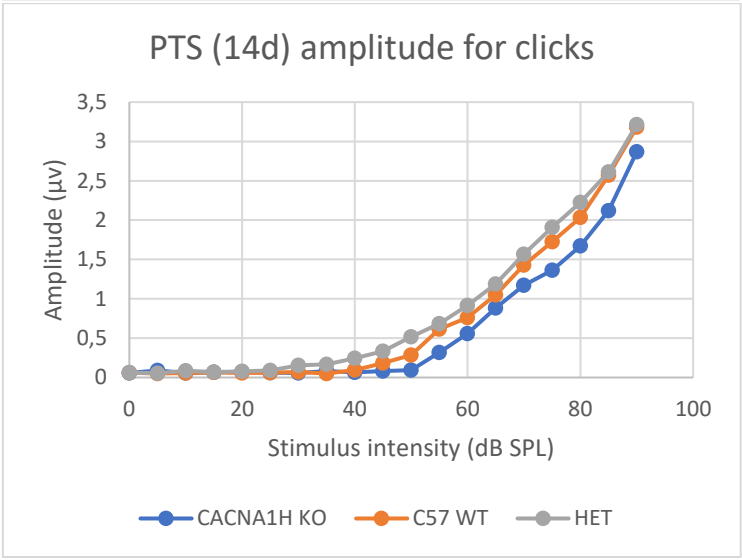

Fig. 5: Amplitudes of wave I of ABR responses of six-week-old mice in PTS 14d conditions (two weeks post noise exposure) for various frequencies of pure tones. A: At 8 kHz, B: at 16 kHz, C: at 24 kHz, D: at 32 kHz, E: for click noises.

In baseline conditions, the KO mice appeared to have larger latencies than WT or HET mice at lower sound intensities; at higher sound intensities the latencies of all groups appeared to be very similar. Meanwhile in post-noising conditions, there appeared to be no recognizable trend, as all the average latencies were very close in value between groups. (Statistical analysis was not performed for amplitudes and latencies of sound waves; however at 90 db, which is the highest sound intensity, all the latencies were extremely close in value in all conditions.)

A

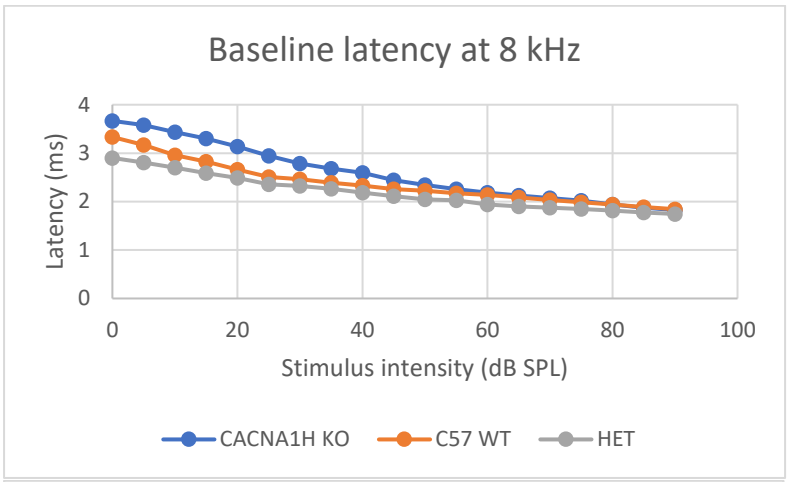

B

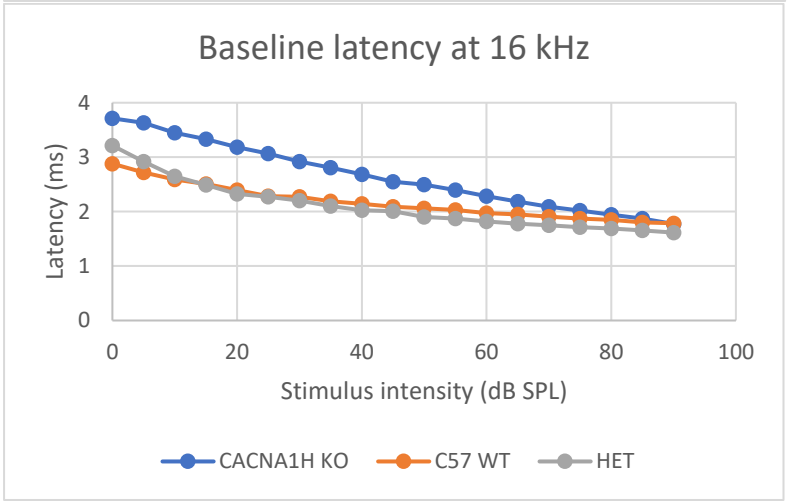

C

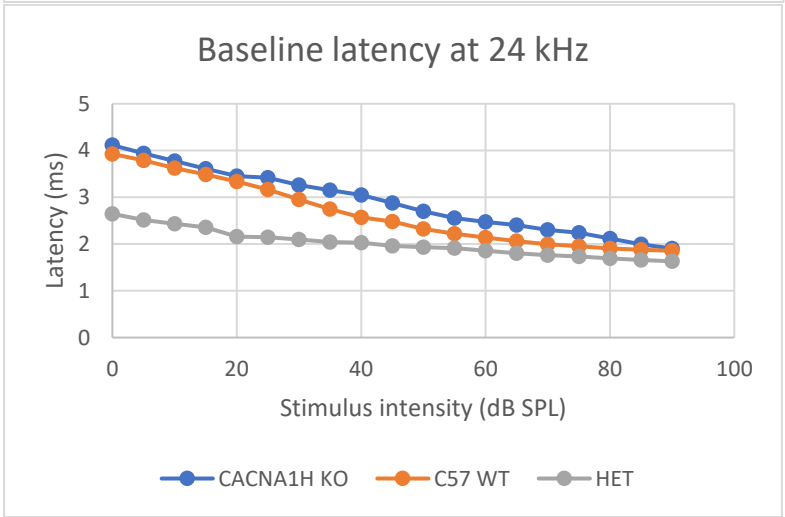

D

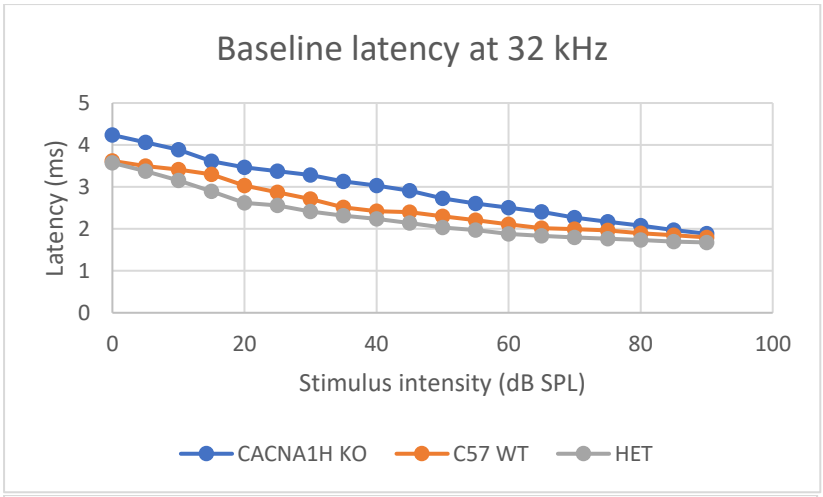

E

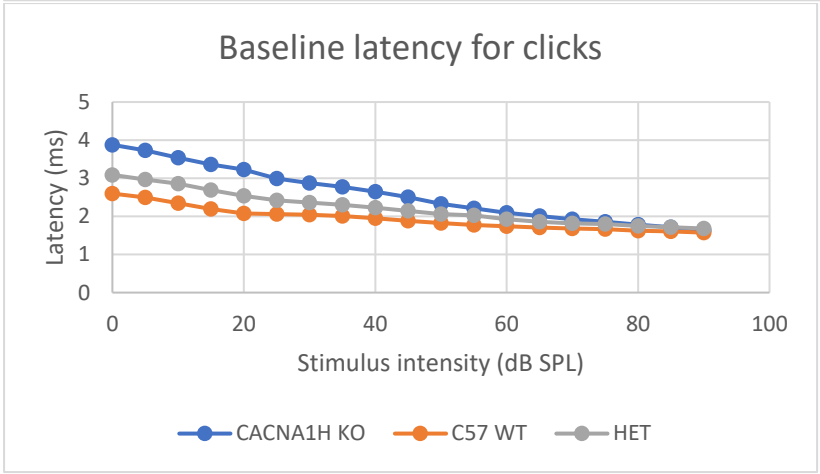

Fig. 6: Latencies of wave I of ABR responses of six-week-old mice in baseline conditions for various frequencies of pure tones. A: At 8 kHz, B: at 16 kHz, C: at 24 kHz, D: at 32 kHz, E: for click noises.

A

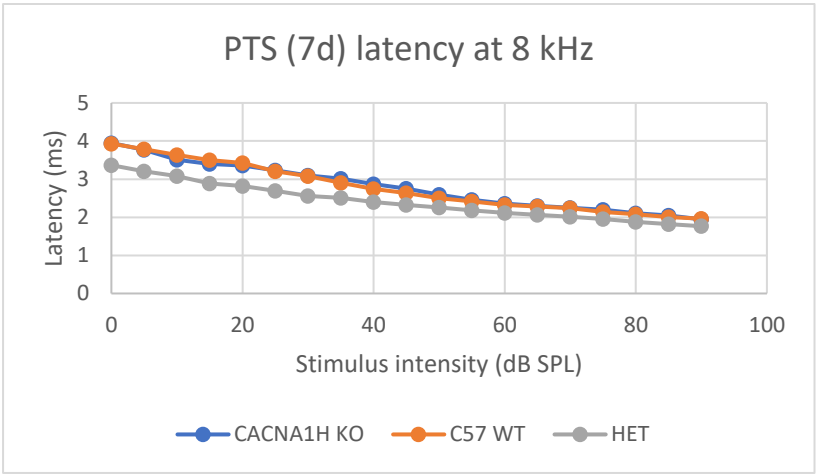

B

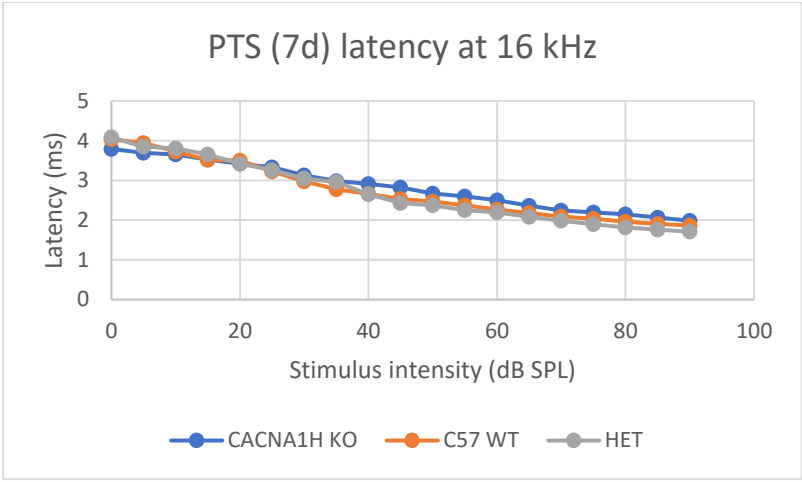
PTS (7d) latency at 16 kHz
Latency (ms)
0
1
2
3
4
5
0
20
40
60
80
100
Stimulus intensity (dB SPL)
CACNA1H KO
C57 WT
HET

C

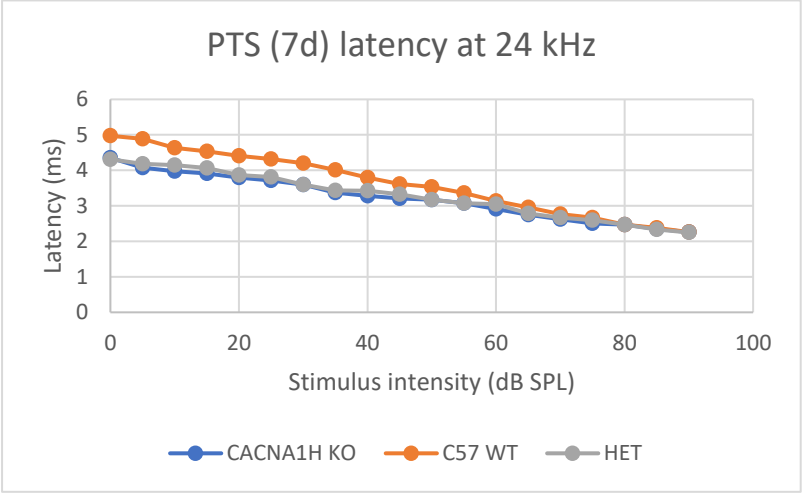
PTS (7d) latency at 24 kHz
Latency (ms)
0
1
2
3
4
5
6
0
20
40
60
80
100
Stimulus intensity (dB SPL)
CACNA1H KO
C57 WT
HET

D

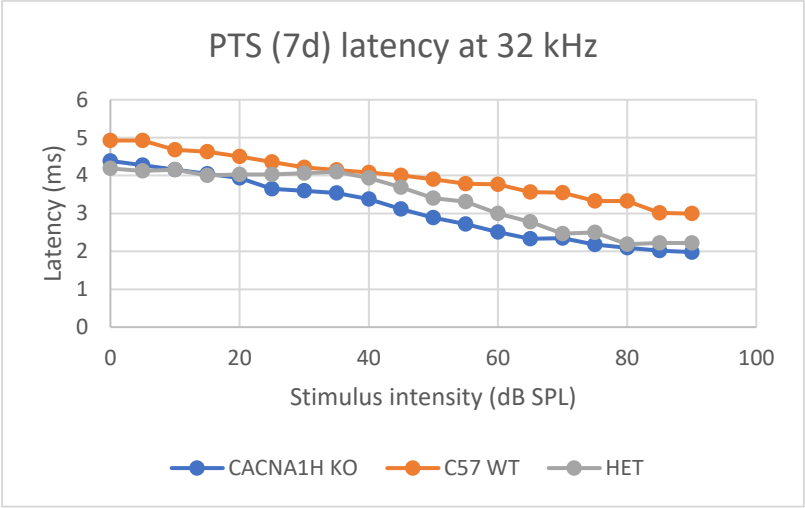
PTS (7d) latency at 32 kHz
Latency (ms)
0
1
2
3
4
5
6
0
20
40
60
80
100
Stimulus intensity (dB SPL)
CACNA1H KO
C57 WT
HET

E

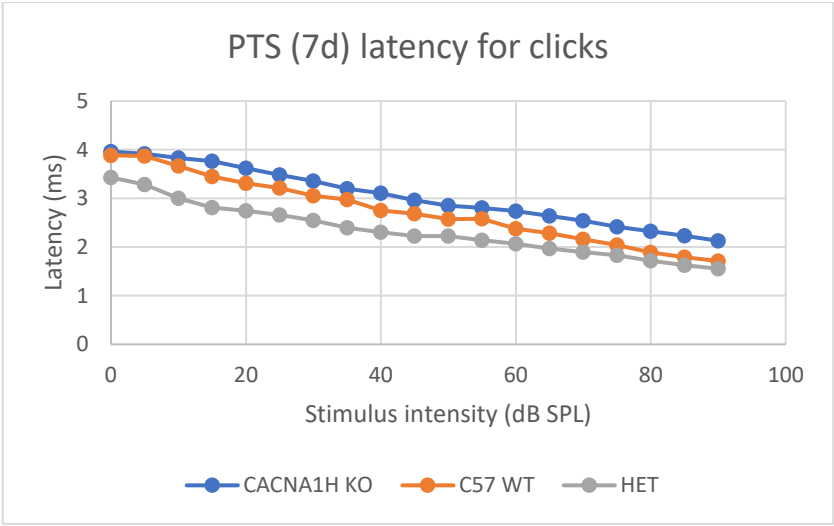

Fig. 7: Latencies of wave I of ABR responses of six-week-old mice in PTS 7d conditions for various frequencies of pure tones. A: At 8 kHz, B: at 16 kHz, C: at 24 kHz, D: at 32 kHz, E: for click noises.

A

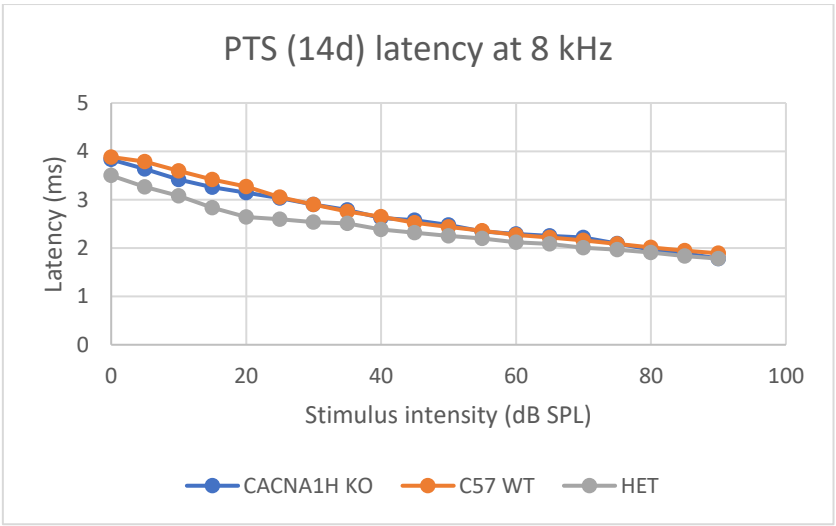

B

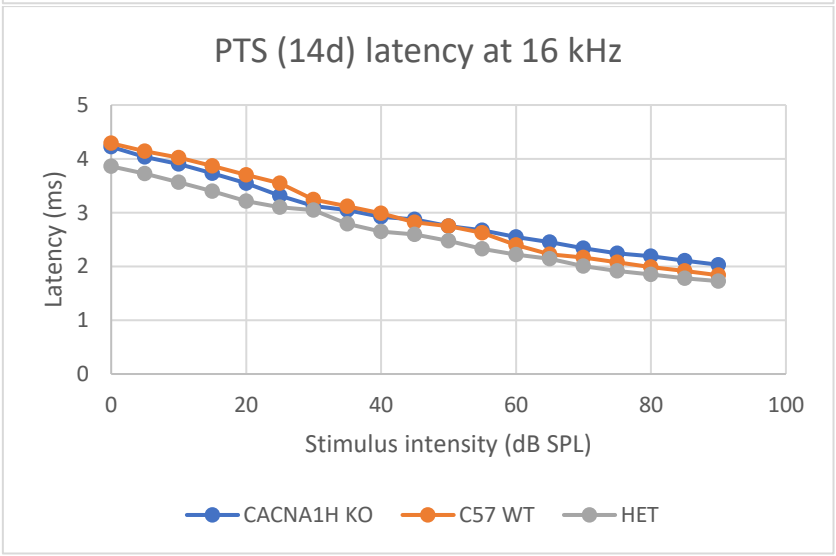

C

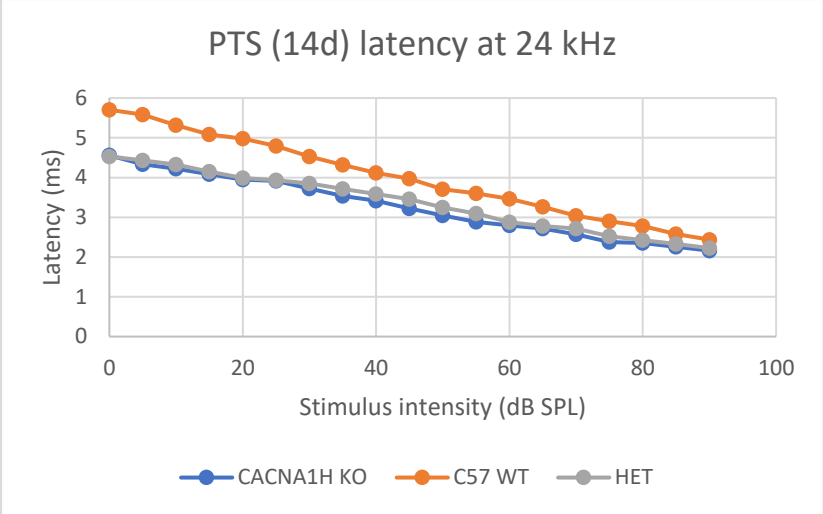

D

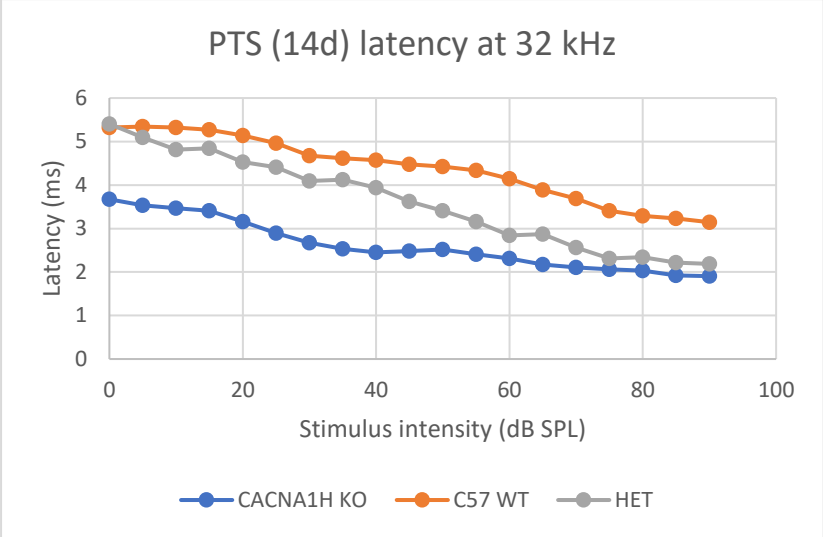

E

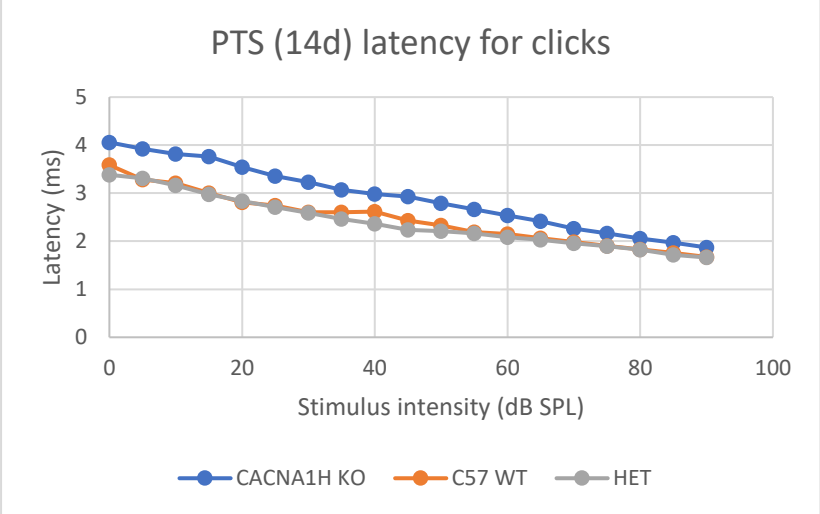

Fig. 8: Latencies of wave I of ABR responses of six-week-old mice in PTS 14d conditions for various frequencies of pure tones. A: At 8 kHz, B: at 16 kHz, C: at 24 kHz, D: at 32 kHz, E: for click noises.

Immunostaining results

A

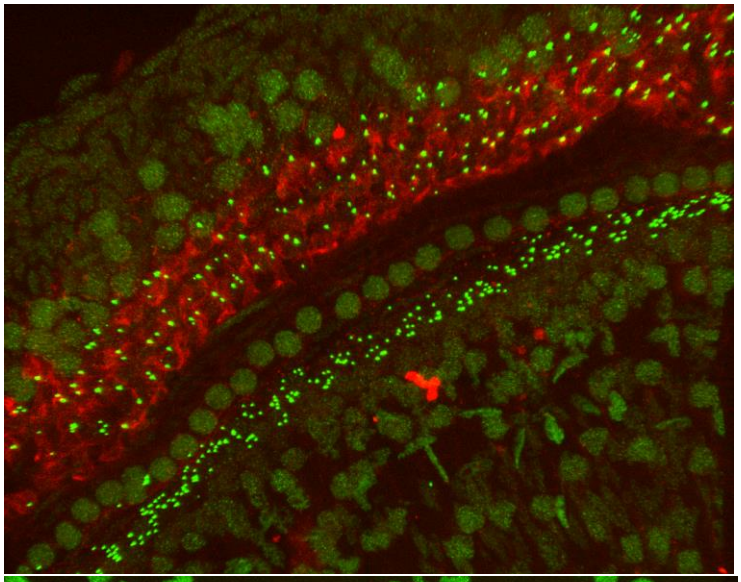

B

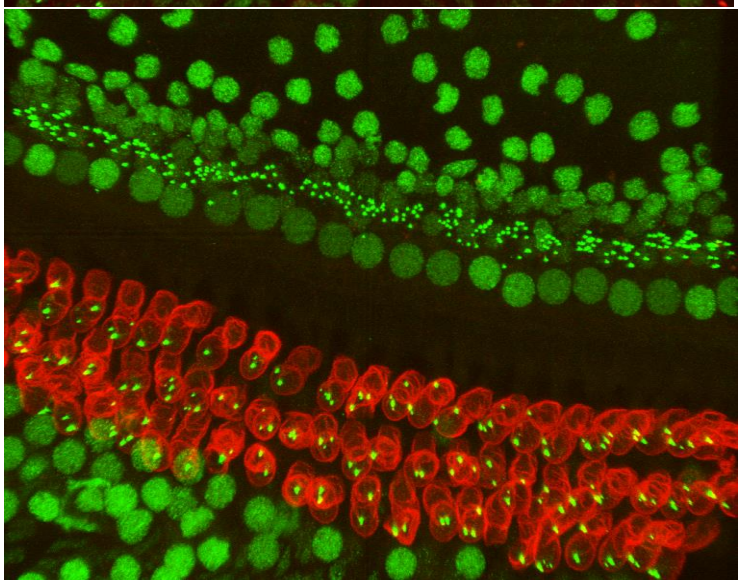

Fig. 9: 8 kHz region of the organ of Corti of a) a WT mouse, b) a KO mouse.

Several WT and KO samples were examined after immunostaining to determine whether noise exposure affects IHCs and synapses differently based on presence or absence of the Cav3.2 channel. The images of the frequency regions of 8, 16, 24 and 32 kHz of each viable sample were examined, and the number of IHCs and their associated synapses were counted.

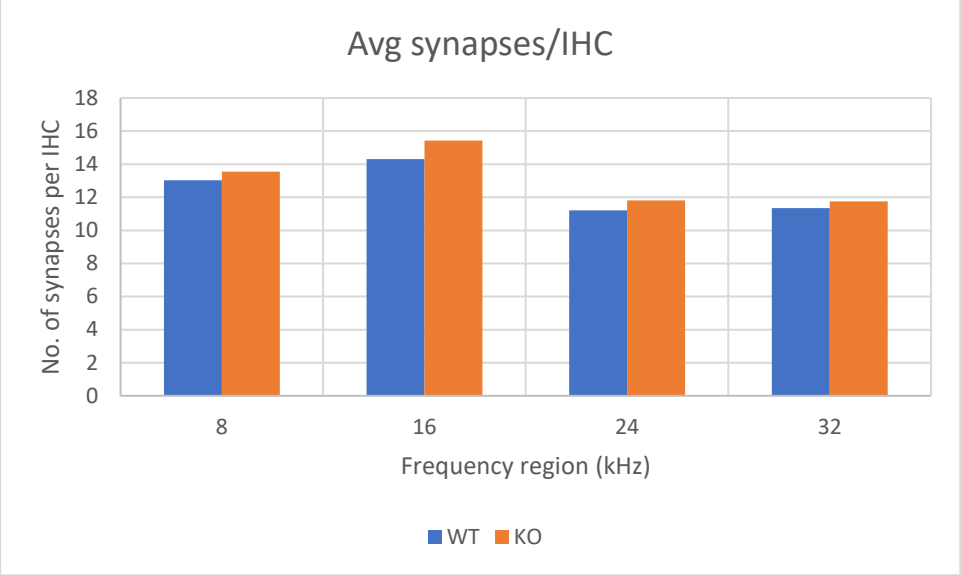

Fig. 10: Average synapse counts per inner hair cell for different frequency regions in the inner ear (8, 16, 24 and 32 kHz).

The average synapse counts per IHC were very similar in WT and KO mice, and in fact, the synapse counts per inner hair cell were slightly higher in KO mice.

Discussion

Since we predicted that lack of Cav3.2 channel would provide some level of protection against noise-induced hearing loss, these results were different from what was anticipated. Firstly, considering there is already such a great disparity in the baseline thresholds of WT, KO and HET mice, and considering KO mice already have very poor hearing in baseline conditions, it is hard to say whether noise exposure affects these mice differently.

From all the above data, it is evident that the absence of the Cav3.2 channel does not appear to offer protection against noise-induced hearing loss. ABR measurements showed that in both HET and KO mice, the effects of noise exposure are more significant than in WT mice. Moreover, even the baseline thresholds are not similar; even six-week-old KO mice prior to noise exposure had significantly higher thresholds than WT and HET mice at all frequencies.

Thus, it is possible that the Cav3.2 calcium channel or the gene encoding for it (CACNA1H) might have another function that is apparently essential to normal hearing. In Lundt et al's 2019 study, it was already observed that Cav3.2 KO mice at the age of five months appeared to have significantly higher auditory thresholds than WT mice[26]. However, this might have been due to the absence of the Cav3.2 channel accelerating age-related hearing loss because the background strain of the mice used shows greater ARHL. Thus, for this particular study, the mice used were about six weeks old – the age at which the auditory system is fully developed. Despite this, the KO mice appeared to have significantly worse hearing, and therefore it can be inferred that the Cav3.2 channel contributes in some way to normal auditory function. Judging by the results of this study, as well as prior data such as from Lundt's study, the Cav3.2 channel might have a role in development of the auditory system from birth.

It was also observed from the cell count data that KO mice appear to have a similar number of synapses per IHC to WT mice, not less as was expected. Thus, it seems apparent that KO mice

are not much more susceptible to synapse or inner hair cell damage caused by noise exposure than WT mice. However, there are a few concerns inherent with this conclusion. Perhaps the most important of these is that no baseline samples (prior to noise exposure) were immunostained, observed or counted. Thus there is no way to observe the extent of damage caused to the cells or synapses due to noise exposure. This oversight can be corrected in future studies by studying cochlea of the mice before and after noise exposure and comparing hair cell and synapse counts.

These results do not make it clear which of the sensorineural structures being affected causes the auditory deficit. ABRs simply show the fact that hearing is damaged, but not which part of the inner ear is damaged (i.e., IHCs, OHCs or SGNs). Thus, further studies need to be conducted at a histological and molecular level to determine what is the exact nature of hearing damage caused by absence of the Cav3.2 channel. Performing additional physiological tests (such as distortion product otoacoustic emissions, or DPOAE tests) as well as locating the channel to other inner ear cells (through procedures such as fluorescence in situ hybridization or FISH) can shed some light on why knockouts have elevated thresholds and where the channel is essential for hearing.

Another interesting finding that may be worth speculation is the observation that in baseline conditions, HET mice seem to have lower auditory thresholds, as well as higher wave I amplitudes, than WT mice. This may be due to some background characteristic of either the WT strain or KO strain (such as a propensity for accelerated age-related hearing loss). For any further speculation to be done, cochleae of the HET mice also need to be examined both prior to and following noise exposure, as well as further ABR experiments on them.

References

1. The European environment - Publications Office of the EU. Accessed July 12, 2021. https://op.europa.eu/en/publication-detail/-/publication/b312a176-1b69-11ea-8c1f-01aa75ed71a1/language-en

2. Agrawal Y, Platz EA, Niparko JK. Prevalence of hearing loss and differences by demographic characteristics among US adults: Data from the National Health and Nutrition Examination Survey, 1999-2004. *Archives of Internal Medicine*. 2008;168(14):1522-1530. doi:10.1001/ARCHINTE.168.14.1522

3. Kryter KD, Ward WD, Miller JD, Eldredge DH. Hazardous Exposure to Intermittent and Steady-State Noise. *The Journal of the Acoustical Society of America*. 2005;39(3):451. doi:10.1121/1.1909912

4. Clark WW. Recent studies of temporary threshold shift (TTS) and permanent threshold shift (PTS) in animals. *The Journal of the Acoustical Society of America*. 1998;90(1):155. doi:10.1121/1.401309

5. Bramhall N, Beach EF, Epp B, et al. The search for noise-induced cochlear synaptopathy in humans: Mission impossible? *Hearing Research*. 2019;377:88-103. doi:10.1016/J.HEARES.2019.02.016

6. Bohne BA, Harding GW, Lee SC. Death pathways in noise-damaged outer hair cells. *Hearing Research*. 2007;223(1-2):61-70. doi:10.1016/J.HEARES.2006.10.004

7. Mcgill TJI, Schuknecht HF. Human cochlear changes in noise induced hearing loss. *The Laryngoscope*. 1976;86(9):1293-1302. doi:10.1288/00005537-197609000-00001

8. Frye MD, Ryan AF, Kurabi A. Inflammation associated with noise-induced hearing loss. *The Journal of the Acoustical Society of America*. 2019;146(5):4020. doi:10.1121/1.5132545

9. Yamane H, Nakai Y, Takayama M, Iguchi H, Nakagawa T, Kojima A. Appearance of free radicals in the guinea pig inner ear after noise-induced acoustic trauma. *European Archives of Oto-Rhino-Laryngology 1995 252:8*. 1995;252(8):504-508. doi:10.1007/BF02114761

10. Fridberger A, Flock Å, Ulfendahl M, Flock B. Acoustic overstimulation increases outer hair cell Ca2+ concentrations and causes dynamic contractions of the hearing organ. *Proceedings of the National Academy of Sciences*. 1998;95(12):7127-7132. doi:10.1073/PNAS.95.12.7127

11. Orrenius S, Zhivotovsky B, Nicotera P. Regulation of cell death: the calcium–apoptosis link. *Nature Reviews Molecular Cell Biology 2003 4:7*. 2003;4(7):552-565. doi:10.1038/nrm1150

12. Kujawa SG, Liberman MC. Adding Insult to Injury: Cochlear Nerve Degeneration after "Temporary" Noise-Induced Hearing Loss. *Journal of Neuroscience*. 2009;29(45):14077-14085. doi:10.1523/JNEUROSCI.2845-09.2009

13. Hu N, Rutherford MA, Green SH. Protection of cochlear synapses from noise-induced excitotoxic trauma by blockade of Ca2+-permeable AMPA receptors. *Proceedings of the National Academy of Sciences*. 2020;117(7):3828-3838. doi:10.1073/PNAS.1914247117

14. Vicente-Torres MA, Schacht J. A BAD link to mitochondrial cell death in the cochlea of mice with noise-induced hearing loss. *Journal of Neuroscience Research*. 2006;83(8):1564-1572. doi:10.1002/JNR.20832

15. Pujol R, Rebillard G, Puel J-L, Lenoir M, Eybalin M, Recasens M. Glutamate Neurotoxicity in the Cochlea: A Possible Consequence of Ischaemic or Anoxic Conditions Occurring in Ageing. *http://dx.doi.org/103109/00016489109127253*. 2009;111(S476):32-36. doi:10.3109/00016489109127253

16. Pangrsic T, Singer JH, Koschak A. Voltage-Gated Calcium Channels: Key Players in Sensory Coding in the Retina and the Inner Ear. *https://doi.org/101152/physrev000302017*. 2018;98(4):2063-2096. doi:10.1152/PHYSREV.00030.2017

17. Chen WC, Xue HZ, Hsu YL, Liu Q, Patel S, Davis RL. Complex distribution patterns of voltage-gated calcium channel α-subunits in the spiral ganglion. *Hearing Research*. 2011;278(1-2):52-68. doi:10.1016/J.HEARES.2011.01.016

18. Li Y, Liu H, Giffen KP, Chen L, Beisel KW, He DZZ. Transcriptomes of cochlear inner and outer hair cells from adult mice. *Scientific Data 2018 5:1*. 2018;5(1):1-12. doi:10.1038/sdata.2018.199

19. Dou H, Vazquez AE, Namkung Y, et al. Null Mutation of α 1D Ca 2+ Channel Gene Results in Deafness but No Vestibular Defect in Mice. *Journal of the Association for Research in Otolaryngology 2004 5:2*. 2004;5(2):215-226. doi:10.1007/S10162-003-4020-3

20. Platzer J, Engel J, Schrott-Fischer A, et al. Congenital Deafness and Sinoatrial Node Dysfunction in Mice Lacking Class D L-Type Ca2+ Channels. *Cell*. 2000;102(1):89-97. doi:10.1016/S0092-8674(00)00013-1

21. Brandt A, Striessnig J, Moser T. CaV1.3 Channels Are Essential for Development and Presynaptic Activity of Cochlear Inner Hair Cells. *Journal of Neuroscience*. 2003;23(34):10832-10840. doi:10.1523/JNEUROSCI.23-34-10832.2003

22. Waka N, Knipper M, Engel J. Localization of the calcium channel subunits Cav1.2 (α1C) and Cav2.3 (α1E) in the mouse organ of Corti. *Histology and Histopathology*. 2003;18(4):1115-1123. doi:10.14670/HH-18.1115

23. Zamponi GW, Striessnig J, Koschak A, Dolphin AC. The Physiology, Pathology, and Pharmacology of Voltage-Gated Calcium Channels and Their Future Therapeutic Potential. *Pharmacological Reviews*. 2015;67(4):821-870. doi:10.1124/PR.114.009654

24. Bernal Sierra YA, Haseleu J, Kozlenkov A, Bégay V, Lewin GR. Genetic Tracing of Cav3.2 T-Type Calcium Channel Expression in the Peripheral Nervous System. *Frontiers in Molecular Neuroscience*. 2017;10:70. doi:10.3389/FNMOL.2017.00070

25. Inagaki A, Ugawa S, Yamamura H, Murakami S, Shimada S. The CaV3.1 T-type Ca2+channel contributes to voltage-dependent calcium currents in rat outer hair cells. *Brain Research*. 2008;1201:68-77. doi:10.1016/J.BRAINRES.2008.01.058

26. Lundt A, Seidel R, Soós J, et al. Cav3.2 T-Type Calcium Channels Are Physiologically Mandatory for the Auditory System. *Neuroscience*. 2019;409:81-100. doi:10.1016/J.NEUROSCIENCE.2019.04.024

27. Reijntjes DOJ, Lee JH, Park S, et al. Sodium-activated potassium channels shape peripheral auditory function and activity of the primary auditory neurons in mice. *Scientific Reports 2019 9:1*. 2019;9(1):1-18. doi:10.1038/s41598-019-39119-z

28. JEWETT DL, WILLISTON JS. AUDITORY-EVOKED FAR FIELDS AVERAGED FROM THE SCALP OF HUMANS. *Brain*. 1971;94(4):681-696. doi:10.1093/BRAIN/94.4.681

29. J K, I S, JT R, MA S, RC F. A physiological and behavioral system for hearing restoration with cochlear implants. *Journal of neurophysiology*. 2016;116(2):844-858. doi:10.1152/JN.00048.2016

30. Barone CM, Douma S, Reijntjes DOJ, et al. Altered cochlear innervation in developing and mature naked and Damaraland mole rats. *Journal of Comparative Neurology*. 2019;527(14):2302-2316. doi:10.1002/CNE.24682

31. Reijntjes DOJ, Breitzler JL, Persic D, Pyott SJ. Preparation of the intact rodent organ of Corti for RNAscope and immunolabeling, confocal microscopy, and quantitative analysis. *STAR Protocols*. 2021;2(2):100544. doi:10.1016/J.XPRO.2021.100544

32. Anti-Cav3.2 (CACNA1H) Antibody | #ACC-025 | Alomone Labs. Accessed July 12, 2021. https://www.alomone.com/p/anti-cav3-2-2/ACC-025